A NEW CONCEPT OF FAST MOBILE ROVER WITH IMPROVED STABILITY ON ROUGH TERRAIN

J.C. Fauroux[1], J. Dakhlallah, B.C. Bouzgarrou
Clermont University, French Institute for Advanced Mechanics (IFMA), LaMI
B.P. 10448, 63000 CLERMONT-FERRAND, France

Summary: This paper presents a new concept of mobile robot capable to cross all-terrain obstacles at high speed. Based on innovative suspensions that have two degrees of freedom per wheel, it relies on horizontal passive damping capacities to cross very steep and high obstacles. This result was obtained by multibody simulation. A single-wheel and a double-wheel model model are presented and several configurations are tested.

Keywords: mobile robots, high speed obstacle clearing, wheel impact, active and reactive suspension design, dynamic modeling, stability control

1 Introduction

Crisis conditions such as earthquake rescuing or de-mining operations require fast deployment and rapid analysis of broad areas of unstructured environment. In this context, a float of mobile, fast and inexpensive robots could be of great usefulness for extensive scanning of the area.

One important problem to address is mobility on irregular grounds at fast speed. The FAST program of the French National Agency of Research is dedicated to design and control an innovative mobile robot of about 1m and 150kg, capable to move at 10m/s on irregular grounds. Work is in progress on innovative mechanical architectures, as well as advanced control strategies. This paper focuses on straight line motion and pitch angle stability during dynamic crossing of steep obstacles at 10 m/s.

Sections 2 and 3 introduce the addressed types of grounds and the existing all-terrain suspensions. Section 4 presents a first model of a single wheel that is useful to understand contact modeling and the behavior of a rolling body on an obstacle. Virtual obstacle crossing shows that important horizontal forces result from the contact and shock of the wheel rolling on the obstacle. For this reason, an innovative concept is introduced in Section 5 : suspensions with two Degrees Of Freedom (DOF). Sections 6 and 7 present a 2D model of a complete vehicle rolling on an obstacle and the preliminary obtained results.

1 Corresponding author : fauroux@ifma.fr, Tel : 00.33.4.73.28.80.50

2 Addressed types of grounds and obstacles

The shape of ground can be modeled with several degrees of detail, depending on the size of the vehicle. Figure 1 presents two types of natural grounds. A structured ground (a) can be represented as a mathematical surface that is continuous of order 0 (C^0, no hole), 1 (C^1, tangential continuity) and possibly higher orders (C^2 for curvature continuity). On the contrary, an unstructured ground such as the one shown in (b) contains many bumps, holes and trees. As the trees give an idea of the scale, one can understand that a vehicle of 1m cannot take every position: at least the location of the trees are forbidden for the vehicle, as well as the cracks and cliffs of the landscape.

(a)

(b)

Figure 1. Two types of natural grounds.(a) Structured ground. (b) Unstructured ground.

This introduces the notion of obstacle (Figure 2) as a local perturbation in the general shape of the ground. Positive obstacles (a,b,c) lay above the ground average surface whereas negative obstacles (d,e,f) lay beneath. Obstacles (a,d) that cannot be crossed by the considered vehicle are treated as walls (a) or holes (d) and represent a forbidden zone for the vehicle on the ground, that becomes locally non C^0. This paper will focus on bumps (b,c), of height h. Case (b) will be treated in priority as it can be considered as a worst case of (c) because a wheel is designed to roll preferably on a C^1 surface.

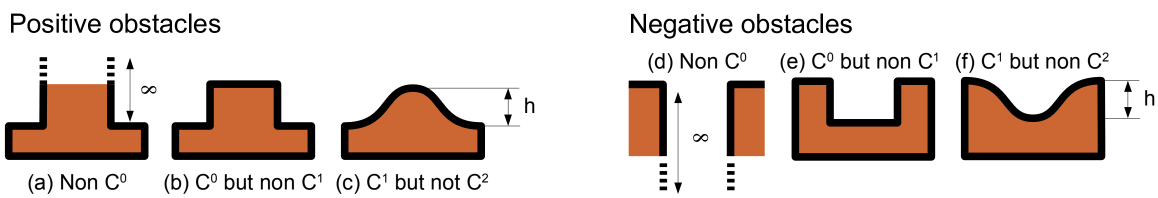

Figure 2. Six types of positive and negative obstacles.

Obstacle that respect conditions (1) and (2) are considered, with r the radius of the wheel.

$$h < r \quad (1)$$

$$h \sim r \quad (2)$$

(1) comes from the geometry of the wheel and means that a given obstacle of height h can be cross-able or not depending on the radius of the wheel of the vehicle. This means that even what is considered as a structured landscape by a man (Figure 1(a)) may become

unstructured for a vehicle of a lower scale. (2) is a rather ambitious objective as most of the wheeled vehicles have difficulties to dynamically cross obstacles as high a 30% of the wheel radius. This can be checked on any bicycle trying to cross a pavement edge. Condition (2) means we want to maximize the crossing capacity of the wheel, mostly by adding appropriate suspensions. It must also be noticed that an obstacle may be easy to cross at speed V_1 and impossible to cross without an accident at speed $V_2 > V_1$. So it is important to keep in mind our objective of 10m/s.

3 Existing all-terrain suspensions

The suspensions of modern vehicles aim to improve dynamics of the vehicle in a wide variety of driving conditions such as loaded/unloaded state, acceleration/braking, straight running/cornering, smooth/uneven road. Depending on the application, all-terrain mobile robots treated in this paper have additional requirements such as running-off-road, crossing obstacles, climbing and running at high speed. According to [Hal95][Rei01], suspensions can be classified in two categories:

- Rigid and semi-rigid axle suspensions (Figure 3a) were the first to appear and are still used on all-terrain vehicles. These suspensions are dedicated to commercial heavy vehicles. They can have a whole series of disadvantages that are a consideration in passenger cars, but which can be accepted in commercial ones. However, they are more efficient supporting high loads.
- Independent wheel suspensions (Figure 3b) such as double wishbone suspensions, McPherson strut suspension, rear axle trailing-arm suspension, semi-trailing-arm axles, multi-link suspensions, that are supposed to be more comfortable and adjustable.

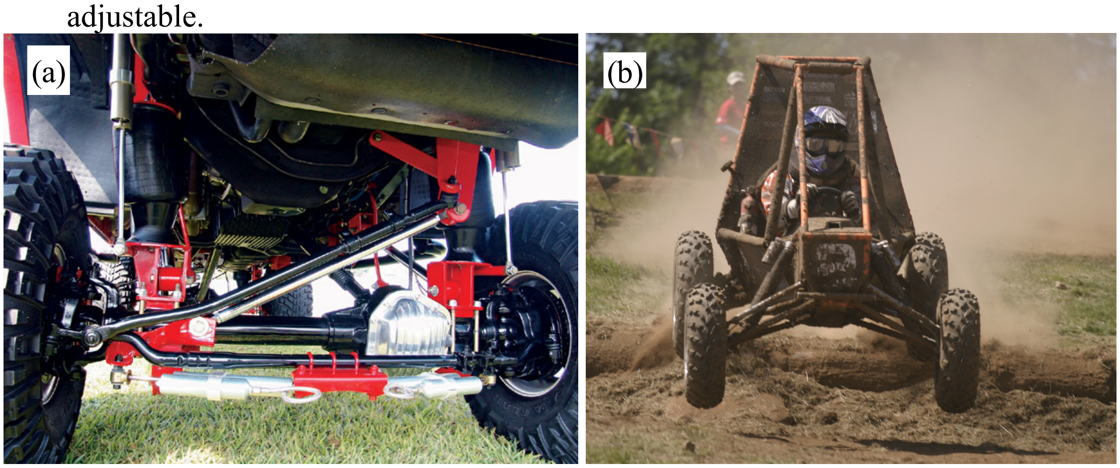

Figure 3. Examples of existing all-terrain suspensions. (a) Ford F350 4x4 rigid axle suspension. (b) Mini-Baja vehicle at Oregon State University with double wishbone suspension.

Some suspensions integrate actuators and are therefore qualified of "active suspensions". Two examples are the Bose suspension [Bos10] (Figure 4a), a McPherson derivative that replaced springs by electromagnetic actuators adapted from loudspeakers, and the Michelin ActiveWheel [Mic08] (Figure 4b), that uses an actuated rack and pinion located inside the rim of the wheel. These two suspensions are interesting to compensate local irregularities on a plain road. As they are active suspension, they require a lot of energy for the suspension actuators as well as a knowledge of the road profile and irregularities. Robustness of the actuators is a critical point in all-terrain and the vertical run of the wheel, limited by the diameter of the wheel in the case of ActiveWheel, should be as long as possible.

(a)

(b)

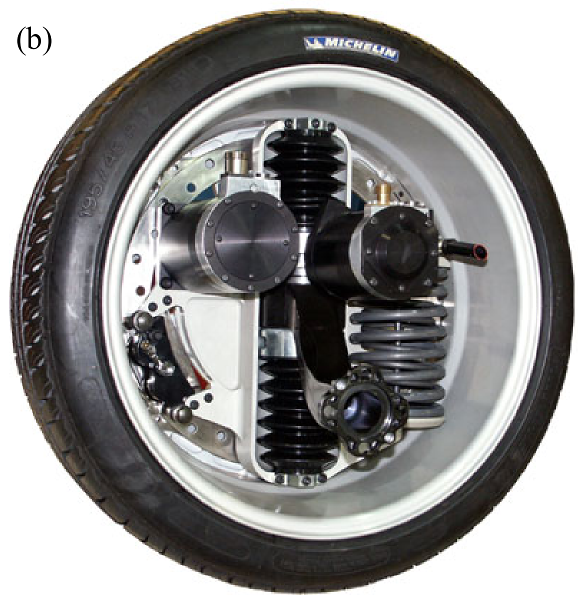

Figure 4. Examples of active suspensions. (a) Bose [Bos10] (b) Michelin ActiveWheel [Mic08].

To our knowledge, it appears that most of the existing suspensions are passive ones. Although they are not as efficient as active suspensions, they have the advantage to be inexpensive, energy efficient, reliable and not to require any knowledge of the environment. In the literature, many patents exist that describe innovative passive suspension systems. In [Che09], a novel suspension system is developed for independent wheel control. The main objective of this system is to provide an independent suspension apparatus for an off-road vehicle that is capable of moving each wheel away and towards a frame or body member of such vehicle. Other works are aimed to adjust vehicle suspension height to provide more ground clearance to the body work of the vehicle [McI09]. Other patented innovations try to improve the performance of a shock absorber [Cox09].

One original system is the suspension with two degrees of freedom presented by Sacli [Sac09]. This patent describes a new suspension architecture which includes two sets of spring-dampers mounted along two different axes: vertical and slightly inclined lateral axes (Figure 5). Such design combines a dive suspension with a roll suspension, including a locking linkage. This invention provides a suspension system that has good bump and dive camber control simultaneously with good roll camber control.

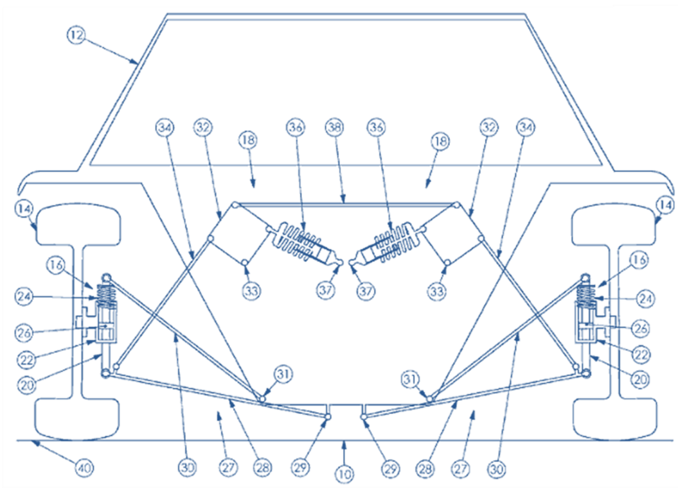

Figure 5. Two degrees of freedom suspension system developed by Sacli [Sac09].

Many existing suspensions replace classical joints by rubber bushings, that allow small displacements in a horizontal plane for a better longitudinal comfort (Figure 6). However, displacements rarely exceed a few millimeters.

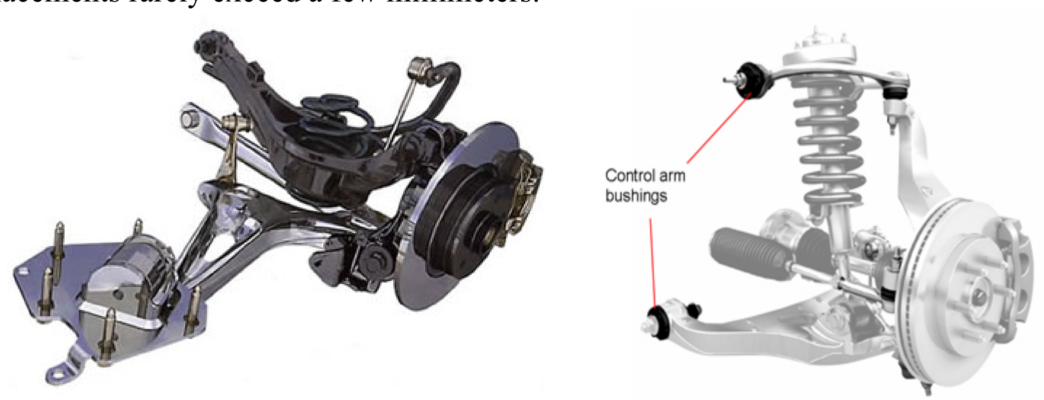

Figure 6.Classical passive suspensions allow short longitudinal motions thanks to rubber bushings. (a) Multi-link suspension. (b) Mc Pherson strut.

From this overview, it is clear that the majority of suspensions, even active ones, do not improve longitudinal stability on rough terrain. Shocks against steep obstacles at high speed modify directly the horizontal vehicle dynamics, which is not addressed by most of the existing suspension systems, as they generally rely on shock absorbers mounted vertically with slight inclinations. For this reason, the main objective of this work is to present a mobile robot equipped with innovative suspensions dedicated to steep obstacle crossing at high speed and as passive as possible.

4 Single wheel model

A preliminary comprehension of fast obstacle crossing is possible with a very simple model. This section presents a study on a single wheel of non deformable material submitted to a constant torque. The wheel rolls with slipping on a flat ground and crosses an obstacle that has an adjustable shape (rectangular on Figure 7). The wheel has center *W*, radius *r*, mass *m* and is submitted to torque *T*. Starting a null speed, it rolls for a run-up distance d_r along the *x* axis and impacts against an obstacle of height *h*. For a given set of parameters (*m*, *r*, *T*, *h*, d_r) the trajectory of the wheel center *W* can be analyzed, as well as the contact forces. The model was created with Adams multibody simulation software (MSC Software, 2008).

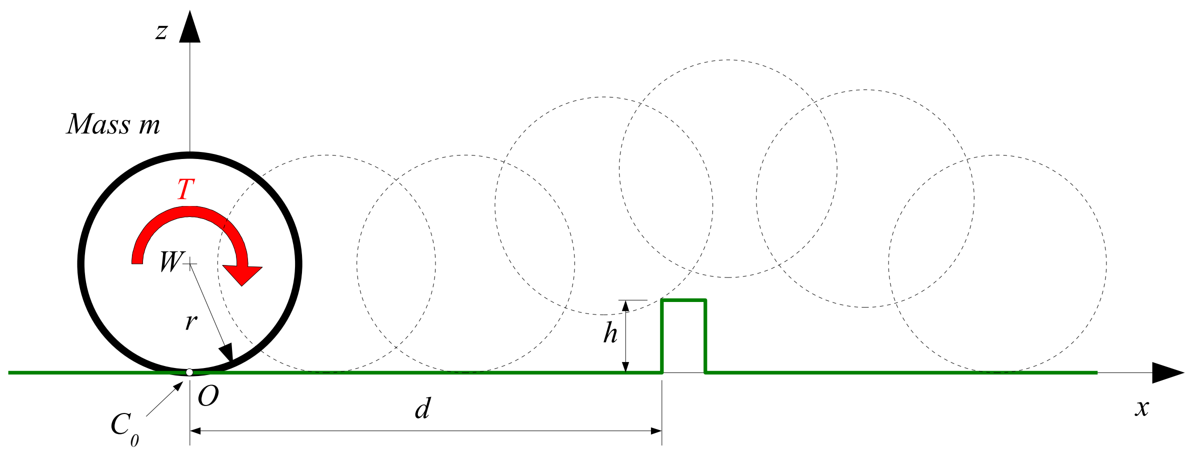

Figure 7. Single wheel model.

Although the wheel is rigid, an elastic unilateral contact is used: the wheel can jump above the ground but penetration under the ground is prevented by an impact normal force given by equation (3) [Msc08]

$$N = Max(0, k.(q_0 - q)^e - C\,\dot{q}\,.STEP(q, q_0 - d, 1, q_0, 0)) \tag{3}$$

where *N* is the normal contact force, *k* is the contact stiffness, q_0-q is the geometric penetration of the wheel into the ground, *e* is a positive exponent, *C* is a damping coefficient, *d* is the penetration distance at which full damping is applied. The term $k.(q_0-q)^e$ is named F_K and represents the elastic part of the normal force, visible on Figure 8(a). The work of F_K is potential energy that is stored at the beginning of the contact and restored at the end of the elastic contact. In case of penetration, F_K may evolve linearly for an exponent value *e = 1* or non linearly otherwise. The rest of the formula corresponds to the damping force F_C , that is proportional to the damping coefficient *C* and to the penetration speed $\dot{q}$. The STEP function is here to apply the maximum damping *C* only after a certain penetration distance *d* (cubic interpolation) and to avoid numerical singularities (Figure 8(b)). The work of F_C is dissipated during contact.

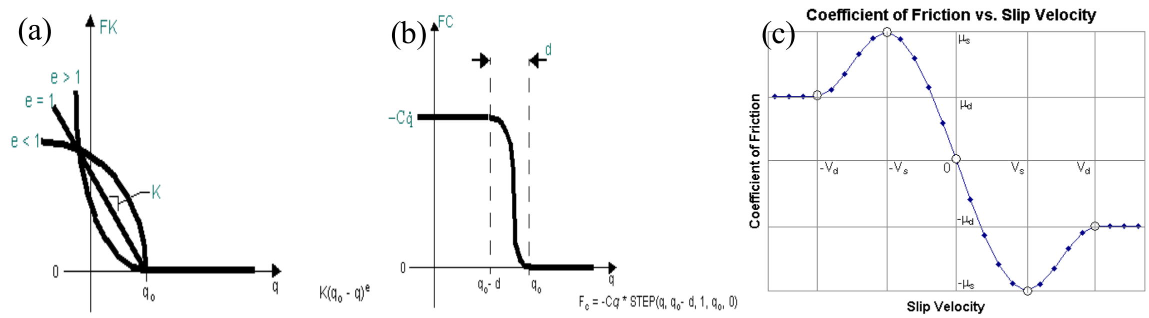

Figure 8. Contact models in Adams multibody software [Msc08]. (a) Elastic part F_K of the normal force. (b) Damping part F_C of the normal force. (c) Friction coefficient.

N can be understood as a penalty that activates as soon as there is geometric penetration between bodies in contact. One should note that double contact appears when the wheel collides against the obstacle: bottom contact with the ground and lateral contact with the obstacle wall. In this case, Adams generates a normal force at each contact point. It was decided to use the generic contact of the solver instead of the tire-contact because the latter requires a very detailed property file for the tire, inspired from Pacejka model [Pac06], which is not defined here in this type of qualitative analysis.

Approximate interference detection is performed by discretizing the two contacting curves into short segments and checking contact for each pair of corresponding segments. The ground curve is defined by a poly-line drawn on a series of parametrized points that can be easily adjusted. Grounds with C^1 continuity can be modeled with a spline curve, although interference detection is made by replacing the smooth curve by a poly-line.

Tangential force T is generated via a Coulomb model base of a variable friction coefficient μ that varies with respect to slip velocity V (Figure 8(c)). The shape of the evolution law is defined by three points : $(0,0)$; (μ_s, V_s) for static friction; and (μ_d, V_d) for dynamic friction. This model is capable to represent the fact that μ_s is generally higher than μ_d. However, it is not realistic at null slipping speed, where friction is null in the Adams model but never null in the real world. But this shape has the advantage to avoid any discontinuity between positive and negative slipping velocities, which improves numerical stability at the price of realism. It means that the wheel will have to slip before that any grip traction can be obtained at the beginning of the simulation.

The chosen reference parameters are the following :

- $m = 5kg$. The vehicle chassis to design will weigh around 100kg. The mass of the wheel is around 5% of the mass of the vehicle.
- $r = 0,25m$, which is the order of magnitude for a small All-Terrain Vehicle (ATV).
- $h = 0,1m$ as the obstacle height.
- $T = 10Nm$ for the driving torque.
- $k = 1E5N/mm$. This value is high, as we want a stiff contact for beginning. Too high values of k may give numerical problems.
- $e = 2$, which corresponds to a stiffening spring. Adams recommend to take a value of 1.5 or higher.

– *C = 100Ns/mm* : low viscous dissipation. The damping coefficient depends highly on the type of ground and is difficult to measure. Adams manual recommends a non null value here for numerical stability (preferably 1% of the stiffness value)
– μ_s = 0.8 and μ_d = 0.7. The static coefficient of a rubber tire on dry macadam is around 1. On natural ground, 0.8 gives a good starting point, although is can be much lower on mud or grounds with low cohesion.
– V_s = *10* mm/s and V_d = *100* mm/s for transition speeds.

A sensitivity study is then performed in order to analyze the influence of several critical parameters.

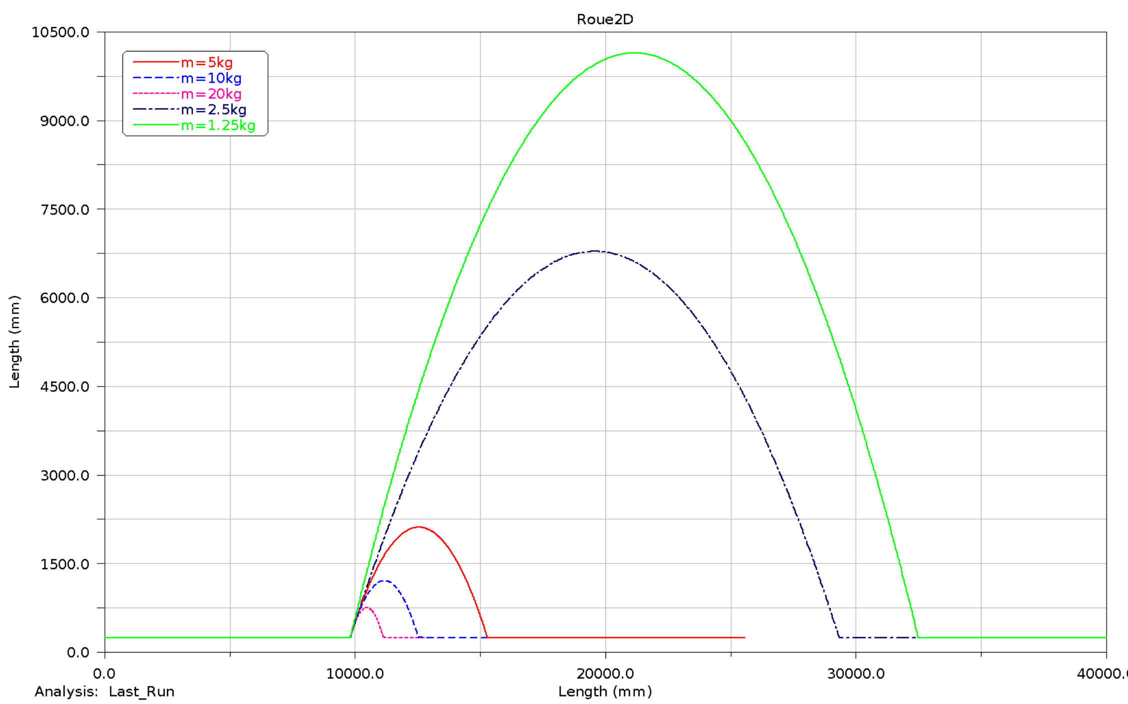

Figure 9. Influence of mass m.

Figure 9 shows that the influence of mass *m* on the balistic trajectory is very high. As expected, a lighter wheel jumps higher and longer. All the trajectories have the same shape but differ from a scale factor.

Figure 10 demonstrates that the obstacle height *h* is a major factor. The wheel crosses the obstacle provided that relation (1) is satisfied. With *h = 260mm*, the wheel rebounds backwards against the obstacle. It appears that *h = 100mm* produces the highest jump whereas *h = 60mm* generates the longest. With higher values of *h*, the jumps is rather short and high. With lower values of *h*, the jumps is rather long and low. All these tendencies look correct and tend to demonstrate the contact model is meaningful.

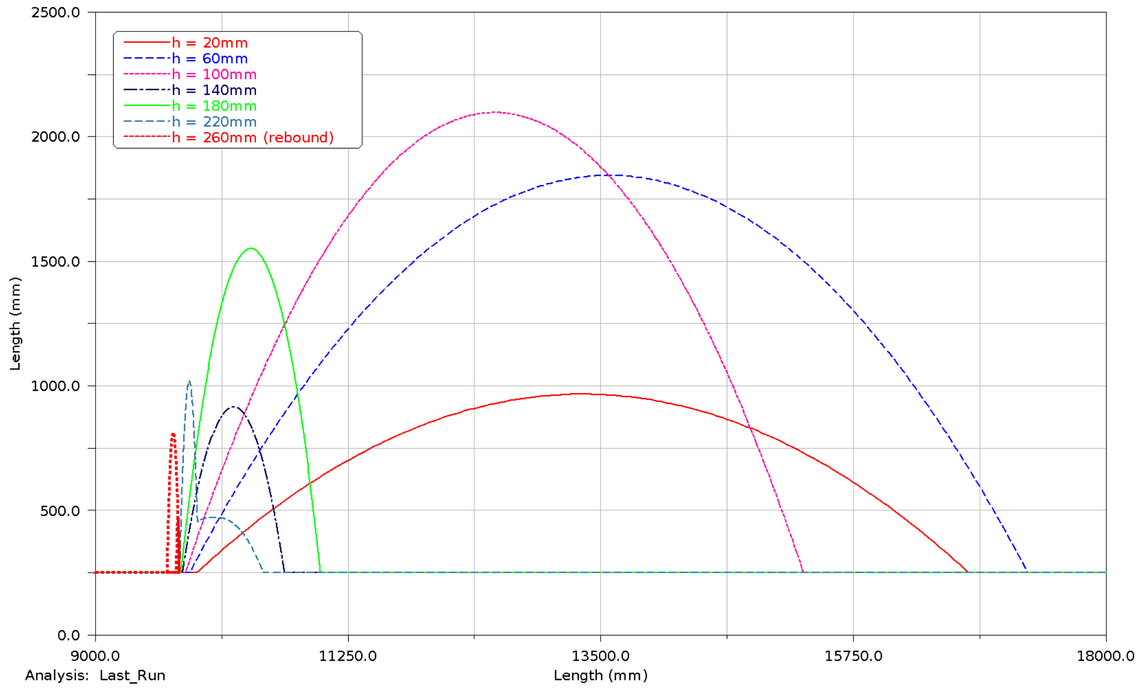

Figure 10. Influence of obstacle height h.

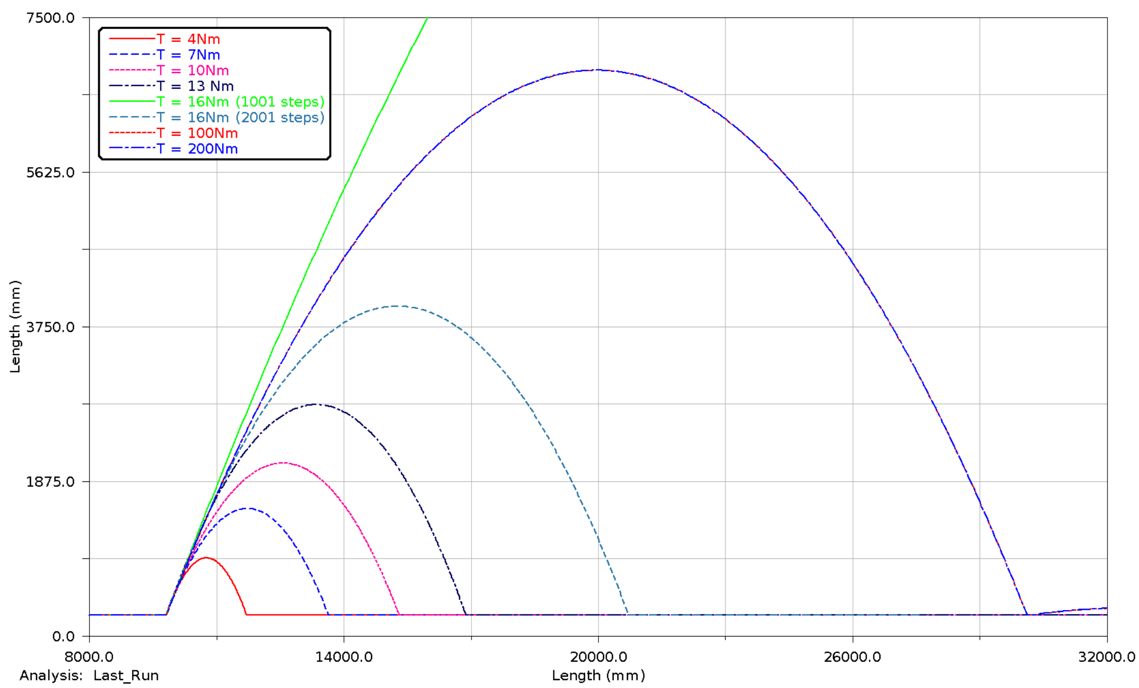

Figure 11. Influence of Torque T.

On Figure 11, results show that higher torques *T* generate bigger jumps, with conservation of the shape and only a scale factor of difference. The curves also exhibits a saturation phenomenon: with extreme values of T (100Nm and 200 Nm), the curves are the same. This means that the contact cannot transmit more tangential force (friction limit). For $T = 16Nm$ also appeared an artefact : the usual time discretization at 1001 steps produced a huge abnormal jump. Using 2001 steps instead led back to a correct result.

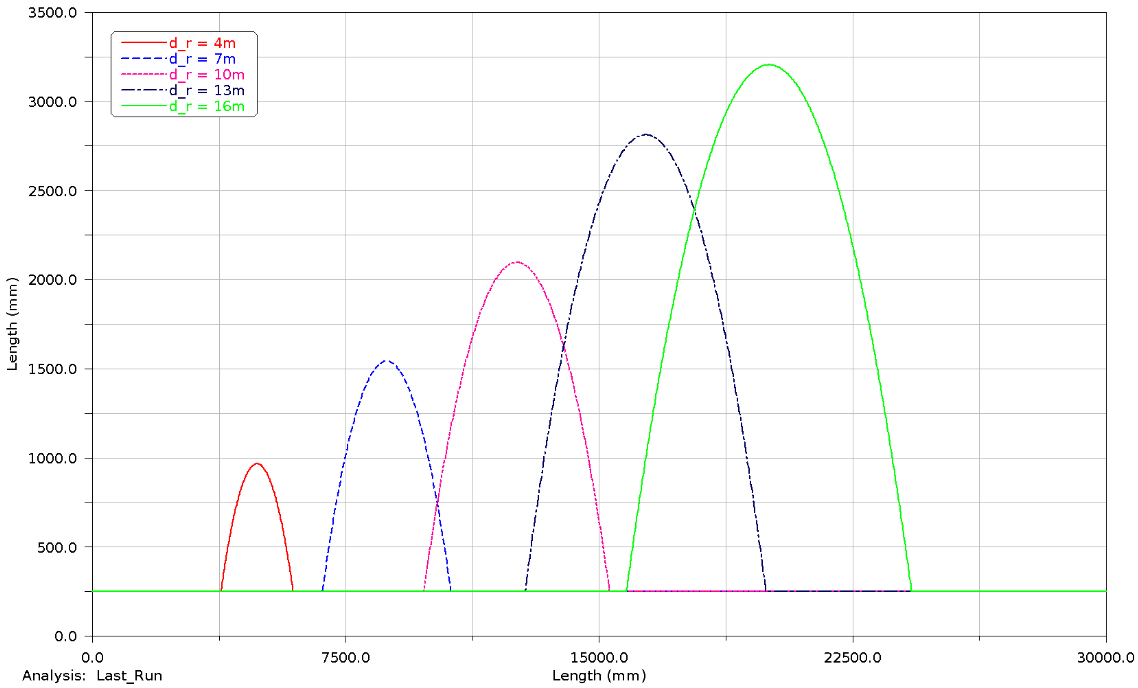

Figure 12. Influence of running distance d_r.

Figure 12 shows 1also the importance of the running distance d_r . The higher the distance, the higher the impact speed and the bigger the jump. All the jumps look homothetic.

But other studies were also performed and demonstrated that:

- The contact stiffness k has not a significant effect on the trajectory provided that it remains inferior to 1E6N/mm. For higher orders, numeric convergence problems tend to appear.
- The exponent e has not a very important effect either. A too low value ($e = 0.25$) generates small oscillations.
- The contact damping coefficient C has a very strong influence: values of 1 and 10 Ns/mm lead to very different trajectories. Above 100Ns/mm, results tend to converge.

5 Innovative suspension

The analysis of a single wheel allowed to check the realism and the limits of the contact modeling in Adams. It also showed that the horizontal forces cannot be neglected anymore with respect to the vertical ones in this type of obstacle crossing. Figure 13 shows the typical profile of the ground we want to address and the horizontal component of the normal vector gives an idea of the intensity of horizontal forces.

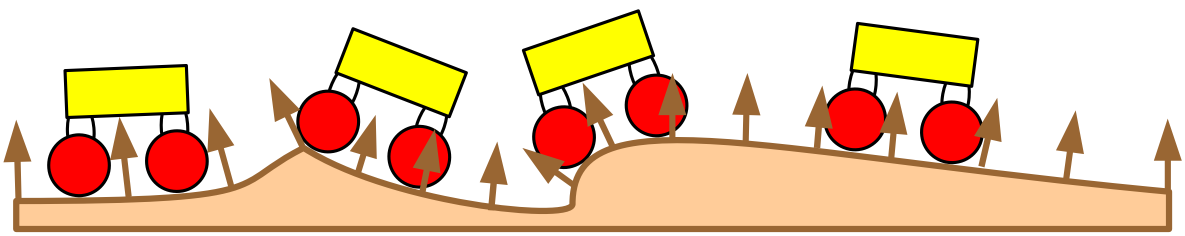

Figure 13. A typical case of ground profile for our robot and the associated normal forces.

The natural consequence of this fact is that new suspensions will have to be designed in order tho absorb both vertical and horizontal contact forces. They could have many different implementations such as the one represented on Figure 14, using two cylinders in parallel, or even two prismatic joint serially connected, such as in the Adams model presented below in Section 6.

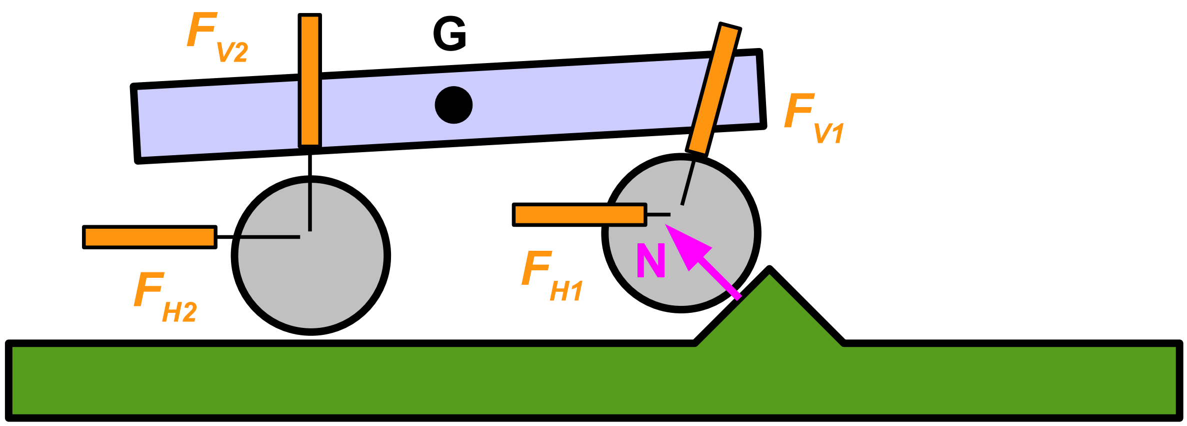

Figure 14. Concept of suspension with 2DOF per wheel.

6 Two-wheel 2D model for pitch stability

The Adams model used to check the interest of 2 DOF suspensions is presented in Figure 15. Ground **0** is modeled by a 20m long plate, with an adjustable block on it for the obstacle. The chassis is made of two weighting spheres **1** and **2** that can be adjusted in mass independently. There were weighting 50 kg each for this work. The bar **3** guides the horizontal translation of cross-shaped sliders **4** and **5**. Two vertical rails **6** and **7** slide through parts **4** and **5** respectively. Wheels $\boldsymbol{W_1}$ and $\boldsymbol{W_2}$ are attached at the bottom of **6** and **7** by a revolute joint. Two needles **8** and **9** are soldered on the wheels as a guiding mark during rotation. All the parts from **3** to **9** have no mass. Although the model has a 3D look for better comprehension, it is a 2D model and is restricted to glide in the sagittal plane XZ.

The horizontal suspension $\boldsymbol{H_1}$ (respectively $\boldsymbol{H_2}$) connects part **3** and **4** (respectively **3** and **5**). The vertical suspension $\boldsymbol{V_1}$ (respectively $\boldsymbol{V_2}$) connects part **4** and **6** (respectively **5** and **7**). All the suspensions include both a spring and a damper. The vertical suspensions are pre-loaded of 500N each in order that the chassis keeps its initial altitude. All the springs have vertical values of 5N/mm. Vertical damping was fixed to 3 Ns/mm whereas horizontal damping was reduced to 1Ns/mm in order to improve shock absorption. The values have an order of magnitude coming from ATV analysis and numerous simulations. The contact parameters are the one described in section 4. Wheels weigh 5kg each and have radius $r_w = 250mm$. The running distance is $d_r = 10m$. The torque T allowing the vehicle to accelerate up to 10m/s after running d_r was determined to be 110Nm for each axle. Lower values of T reach to higher values of d_r. They may also decrease the crossing capacity when the wheel crashes against the obstacle (a high normal force meaning a good lifting tangential force, even with small friction). Obstacle height measures $h = 350mm$, a value that is interesting to push the suspension to its limits.

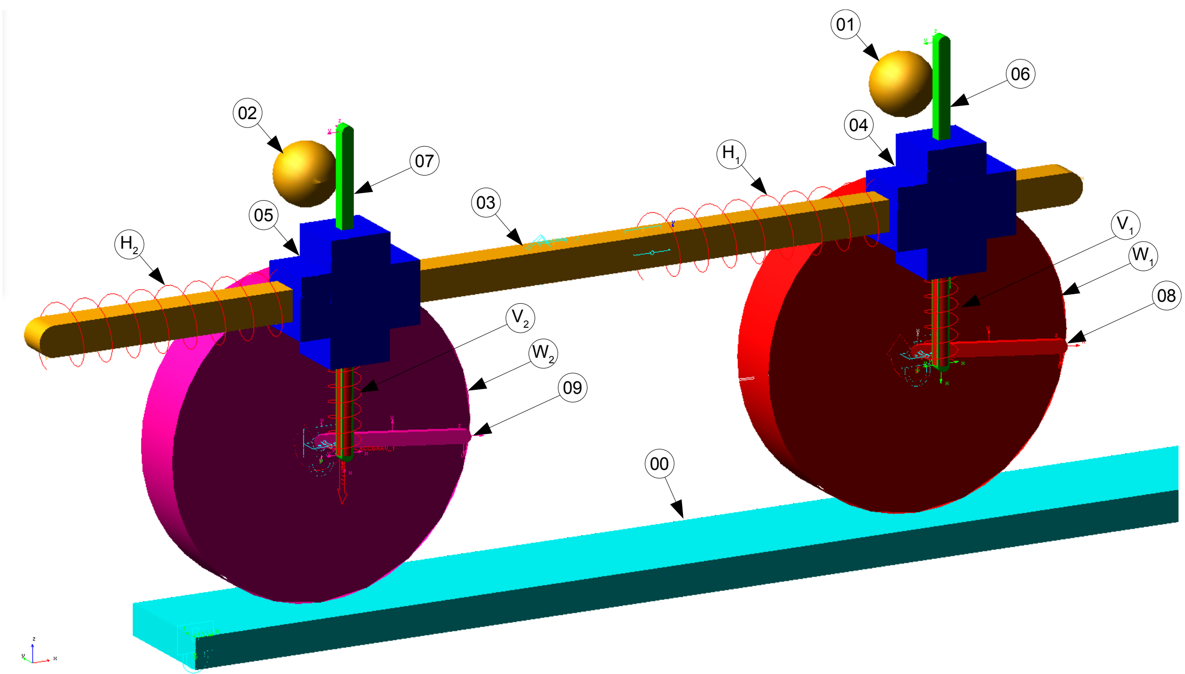

Figure 15. Adams model of a mobile robot with front and rear 2-DOF suspensions.

7 Results

Some significant results are obtained by comparing three configurations of the mobile robot with suspensions including or not a horizontal mobility. The configurations are:

a) Without front horizontal suspension H1, without rear horizontal suspension H2

b) With H1 but not H2

c) With H1 and H2

Motion capture of compared trajectories can be found in Figure 16.

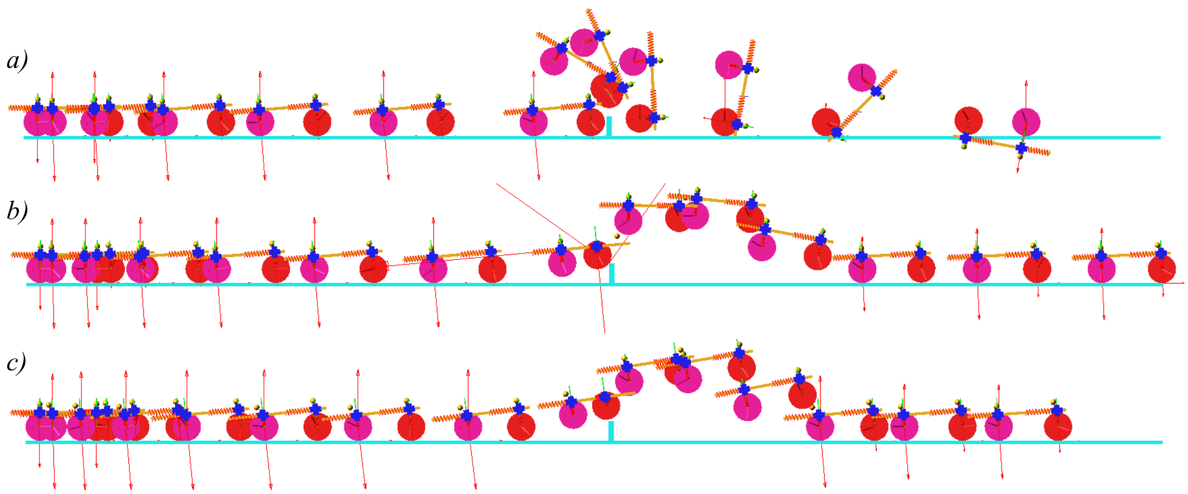

Figure 16. Motion comparison of three configurations with or without horizontal suspensions .

Only b) and c) configurations are stable. The shock with a vertical obstacle creates a horizontal reaction that is absorbed by H1, whereas it perturbs deeply the entire vehicle in case a). Figure 17 represents the compared pitch angles of the vehicles. It allows to differentiate case b), where the vehicle has a maximal pitch angle of -11.5° (nose landing), from case c), where the pitch angle reaches +11.2° (tail landing). Although configurations b) and c) are very close, nose landing is preferable because the driving torque applied to the wheels tends to nullify the pitch angle (auto-stability). In case of tail landing, the driving torque on the rear axle may cause instability. Torque transmission should be stopped or even reversed at landing. For all our models, the torque on rear axle was interrupted after 2s, at a time when the vehicle is in the air. This improved landing stability.

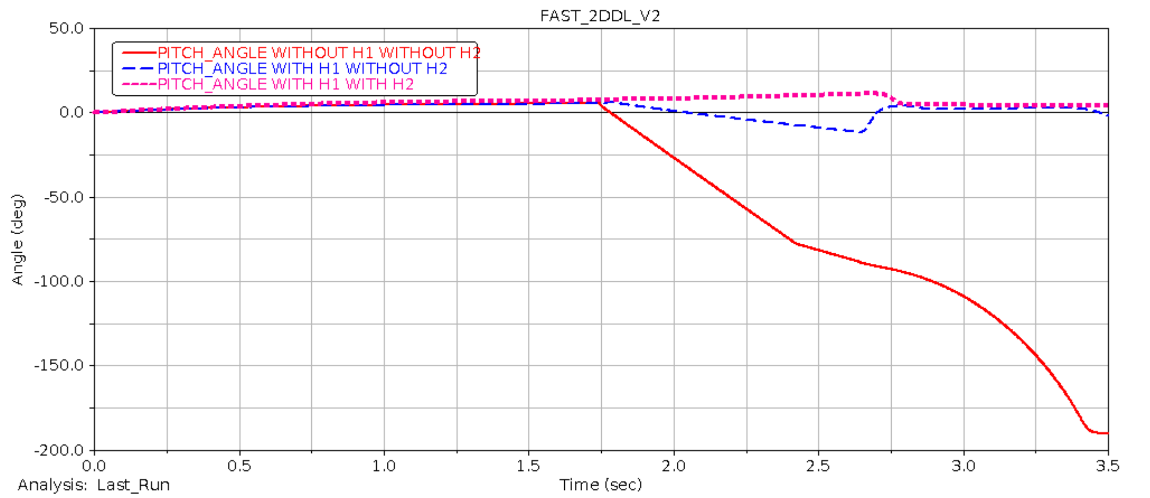

Figure 17. Comparison of pitch angle in three configurations with or without horizontal suspensions .

The horizontal suspension appears to be an important improvement for fast obstacle crossing. However, the front horizontal suspension H_1 has a bigger importance than the rear one H_2. The horizontal forces generally have two peaks corresponding to the first impact on the obstacle and then, to landing. The first peak on F_{H1} is generally higher than on F_{H2}. In case c), there was even no shock at all or the rear wheels against the obstacle (Figure 18). This is why suspension H_1 is vital to improve stability, whereas H_2 is optional. As the frontal shock may lead to loose two-thirds of the kinetic energy and half of the speed of the robot (Figure 18), H_1 must be reinforced relatively to H_2 .

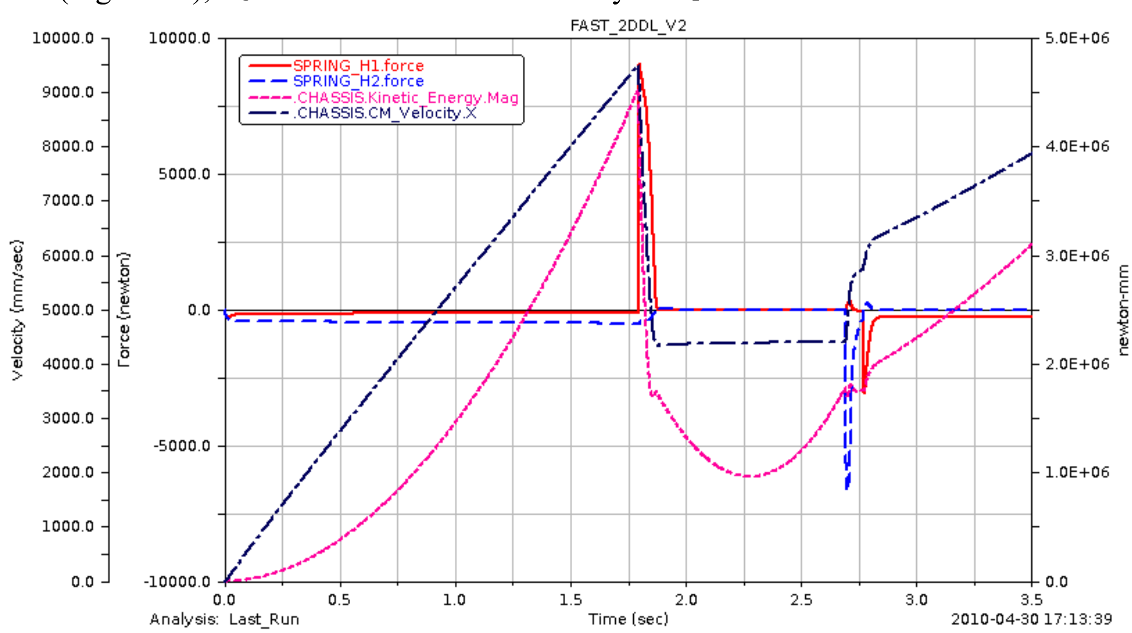

Figure 18. Force values of the horizontal front (H1) and rear (H2) suspensions. The third curve is the kinetic energy of the chassis (wheels not included).

8 Conclusion

This paper presented a new concept of mobile robot suitable for all-terrain obstacle-crossing at high speeds. The originality of this robot is that each wheel is equipped with a 2DOF suspension mechanism that adds a horizontal mobility to the classical vertical one. This supplemental mobility, combined with suitable stiffness and damping, allows to cross an obstacle higher than the radius of the wheel.

This result was obtained by simulation on a multibody software. The contact properties of the wheel on the ground were first checked and characterized with a single wheel model. Then, a two-wheel 2D model was built and several configuration were tested. The ones with horizontal suspension showed very good crossing capacities, although the rear suspension seems to be less useful than the front one. This preliminary result will have to be checked on a prototype, as the shock phenomena are delicate to model acurately with multibody software.

Future work will focus on defining the optimal stiffness and damping coefficients for a given obstacle and vehicle speed. Several options are possible, such as a passive suspension using fixed parameters, a semi-active suspension capable to adjust them with low energy consumption, or even an active suspension capable to inject peaks of force in the suspension when required. The first results are encouraging and show that automatic control scenarios could be defined and implemented in a fast robot in order to make it very stable at speeds previously unachievable.

Acknowledgment

The authors wish to thank the French Research National Agency (ANR) for funding this work inside the FAST (FAST Autonomous Rover) project. They also thank the IFMA students that already contributed on the engineering aspects of this project: Frédéric KREIT, Anthony RIESEMANN, Aurélien AUTHIER, Solange OVAZZA and Richard COUSTURIER.

References

[Bos10] Bose Systems automotive active suspension, retrieved online April 2010, http://www.bosefrance.fr/FR/fr/learning-centre/suspension-problem

[Che09] Cheek E. and al (2009). *Independent Suspension for Lawnmowers, Cutting Decks fnd Off-road Vehicles*. US Patent Application Publication, US 2009/0308040 A1.

[Cox09] Cox C. and al (2009). *Methods and Apparatus for Position Sensitive Suspension Damping*. US Patent Application Publication, US 2009/0277734 A1.

[Dix96] Dixon, J. C. (1996). *Tires, Suspension and Handling*. London: Arnold.

[Hal95] Halconruy T. (1995). *Les liaisons au sol*. Editions E.T.A.I. Boulogne-Billancourt, France

[Kre08] Kreit F. (2008). *Modélisation d'un robot à roues franchissant une bosse et étude de son comportement et de ses paramètres d'influence.* IFMA final year project.

[Mat99] Matschinsky, W. (1999). *Road Vehicle Suspensions*. Professional Engineering Publishing.

[McI09] McIntyre K. (2009). *Suspension Height Adjustment Mechanism*. US Patent Application Publication, US 2009/0261542 A1.

[Mic08] *Michelin Active Wheel , Mondial de l'Auto 2008. Pressbook.* Retrieved online in April 2010 on http://www.michelin.com.

[Msc08] MSC Software Inc. (2008). *Adams 2008 software documentation on CD-ROM*. Chapters "Contact" and "Impact".

[Pac06] Pacejka H.B. (2006). *Tire and Vehicle Dynamics*. SAE Edition, Warrendale, USA. Second edition.

[Rei01] Reimpell J. (2001). *The Automotive Chassis: Engineering Principles*. Elsevier ISBN 0 7506 5054 0.

[Sac09] Sacli M. (2009). *Suspension System Providing Two Degrees of Freedom*. US Patent Application Publication, US 2009/0256326 A1.

[Won08] Wong J.Y. (2008). *Theory of ground vehicles. John Wiley* & Sons, Hoboken, New Jersey, USA. Fourth edition.